

GenzIQA: Generalized Image Quality Assessment using Prompt-Guided Latent Diffusion Models

Diptanu De* Shankhanil Mitra* Rajiv Soundararajan
 Indian Institute of Science, Bengaluru, India
 {diptanude, shankhanilm, rajivs}@iisc.ac.in

Abstract

The design of no-reference (NR) image quality assessment (IQA) algorithms is extremely important to benchmark and calibrate user experiences in modern visual systems. A major drawback of state-of-the-art NR-IQA methods is their limited ability to generalize across diverse IQA settings with reasonable distribution shifts. Recent text-to-image generative models such as latent diffusion models generate meaningful visual concepts with fine details related to text concepts. In this work, we leverage the denoising process of such diffusion models for generalized IQA by understanding the degree of alignment between learnable quality-aware text prompts and images. In particular, we learn cross-attention maps from intermediate layers of the denoiser of latent diffusion models to capture quality-aware representations of images. In addition, we also introduce learnable quality-aware text prompts that enable the cross-attention features to be better quality-aware. Our extensive cross database experiments across various user-generated, synthetic, and low-light content-based benchmarking databases show that latent diffusion models can achieve superior generalization in IQA when compared to other methods in the literature.

1. Introduction

The proliferation of mobile devices with image capturing capabilities has led to an explosion in the number of images captured, stored and shared on various platforms. This has necessitated no reference (NR) image quality assessment (IQA) as an important tool to monitor and control the visual experience. Several NR-IQA algorithms have been designed using both classical [20, 23–25, 36, 45] or deep learning-based approaches [4, 22, 26, 38, 47, 51, 56]. While the classical approaches suffer in their ability to model a wide range of distortions, the deep learning algorithms suffer from a lack of generalization capability. Such models

trained on a large dataset fail to predict image quality on other datasets accurately.

In this connection, multi-modal vision-language models were recently shown to be promising for their generalizability for NR-IQA. In particular, CLIP-IQA [40] shows the promise of vision-language models to predict image quality even in a zero-shot setting. The performance of such a model can achieve very good generalizability on par with IQA specific models through a cost-effective prompt tuning method. These observations motivate the study of how to leverage existing large pretrained models to achieve generalizable NR-IQA.

Recently, several pieces of work are finding that text-to-image diffusion models show superior out of distribution generalization performance compared to vision language models on a variety of image retrieval, recognition and reasoning tasks [8, 13, 18, 21]. This makes them an interesting choice for achieving generalizable NR-IQA. However, it is non-trivial to extend such diffusion models to the perceptual task of IQA. In this work, we propose Generalized IQA (**GenzIQA**) to explore the potential of prompt-guided text-to-image diffusion models for achieving generalizable NR-IQA.

We show that a combination of learning cross-attention between image and quality relevant text features and prompt tuning can achieve far superior generalization than any existing NR-IQA model on a variety of datasets. In particular, the cross-attention features extracted from the intermediate layers of the denoiser of the reverse diffusion process are shown to be extremely useful for IQA. The utility of the cross-attention features for image quality is further enhanced by learning the textual prompts. We conduct a detailed analysis to show that there is a delicate choice of the noise to be added to the image when passed through the diffusion model. We find that the noise level is related to the behavior of the denoiser in the diffusion model. Further, the number of denoising steps also has an impact on the ability of the cross-attention module to extract quality-aware representations.

Our main contributions are summarized below:

* Authors contributed equally to this work

- We demonstrate that latent diffusion models can be effectively adapted for NR-IQA to achieve the best generalizable performance among all existing methods across a variety of IQA datasets.
- We show that quality-aware tuning of cross-attention maps extracted from the intermediate layers of the denoiser in the reverse diffusion process in conjunction with quality-aware learning of context text prompts are necessary to render diffusion models effective for IQA.
- We conduct a detailed analysis of the role of noise added to the latent variable during denoising and find that there exists a delicate relationship between the noise level and the ability of the denoiser for effective IQA.
- Our work shows that pretrained diffusion models can be adapted with very few parameters for the downstream task of IQA to achieve state-of-the-art generalizable performance.

2. Related Work

No-Reference Image Quality Assessment: NR-IQA is a well-studied field over the past two decades. Hand-crafted feature-based methods such as BRISQUE [23], DIVINE [25], BLINDS [32], and NIQE [24, 49] are based upon exploiting the natural scene statistics. CORNIA [45] and HOSA [43] design codebook learning-based methods. These algorithms are generally suited for images with synthetic distortions but fail to generalize well to complex distortions. With the emergence of deep convolutional neural network (CNN) based learning methods, various end-to-end learning methods [15, 51], or methods regressing pretrained CNN features [48, 50] against quality have been designed. Recently, transformer-based models such as MUSIQ [14], TReS [4] and TRIQ [47] have also shown promising performance on both synthetic and in-the-wild IQA tasks. MetalQA [56] proposes meta-learning to capture quality representation in synthetically distorted images and adapts to complex real-world distortions. HyperIQA [38] proposes a hyper network to learn quality estimation module for capturing various distortion and semantic attributes in images.

Towards Generalization in IQA: With the emergence of various IQA databases in recent years, a few methods have tried to address the problem of generalization in IQA. One approach to deal with generalization is by designing self-supervised quality representations on large databases through models such as CONTRIQUE [22], Re-IQA [33], and QPT [54]. CLIP-IQA [40] is a vision-language model that shows very good zero-shot generalization for the IQA task. DEIQT [26] designs an attention-panel decoder learning with limited test data samples. LIQE

[52] trains a clip-based vision language model on six different databases, showing good performance in cross-database settings. TTA-IQA [31] uses the test-time adaptation technique to generalize a pretrained IQA model for different kinds of databases. Recently, GRepQ [37] presents a self-supervised learning method that can lead to generalized quality representations. Despite these efforts, there is a need to consistently achieve better generalization across diverse and complex distortion types.

Diffusion Models for Downstream Tasks: Over the years, diffusion models have emerged as a popular generative tool that can synthesize high-quality images and show superior performance over other generative models such as generative adversarial networks [5]. In order to ensure faster processing, latent diffusion models work on a lower-dimensional space. One such variant named Stable Diffusion [29] has also shown impressive capabilities in generating high-quality images that are consistent with a given text prompt. The application of diffusion models is not only limited to generative tasks. Their impressive capability in several downstream tasks such as classification [18], object detection [21], segmentation [12, 42], and image retrieval [8] has also garnered attention over the years. This popularity in downstream applications has also made the researchers explore the capability of diffusion models for the face IQA task [1]. However, the use of diffusion models for NR-IQA of natural images is still nascent, particularly from the point of view studying generalizability.

3. Image Quality Assessment using Latent Diffusion Models

In this section, we describe how to adapt and finetune a latent diffusion model for the downstream task of IQA. We first discuss some preliminaries of latent diffusion models in Sec. 3.1, followed by the application of latent diffusion models to IQA by learning text-image cross-attention and prompt tuning in Sec. 3.2. Finally, in Sec. 3.3 we analyze the impact of the denoising in the reverse diffusion process on quality estimation.

3.1. Latent Diffusion Model Preliminaries

Latent diffusion models [29] are a class of diffusion models that encode a real image data x onto a low-dimensional latent space z and learn a distribution in the latent space conditioned on a text input y . In particular, the forward process starts at a image latent variable z_0 progressively corrupted by Gaussian noise, and a learned reverse process generates samples from the latent distribution using a denoising model conditioned on y . In latent diffusion models such as the Stable Diffusion [29] model (SDM), the image x is encoded as $z_0 = \varepsilon(x)$, where $\varepsilon(\cdot)$ is a vector

quantized variational autoencoder (VQ-VAE). The generated latent samples are then passed through a decoder for image generation. Given any timestep t , the forward process distorts the latent representation z_0 to a noisy latent z_t as

$$z_t = \sqrt{\bar{\alpha}_t}z_0 + \sqrt{(1 - \bar{\alpha}_t)}\epsilon, \quad (1)$$

where, $\epsilon \sim \mathcal{N}(0, \mathbf{I})$, $\bar{\alpha}_t = \prod_{s=1}^t \alpha_s$, $\alpha_t = 1 - \beta_t$ and $\{\beta\}_{t=1}^T$ are the noise variances at every timestep $t \in \{1, 2, \dots, T\}$ in the forward process. In the reverse process, the denoising autoencoder $\epsilon_\theta(\cdot)$ takes in the noisy latent z_t , timestep variable t and the conditional variable y to estimate the additive noise in the forward process.

Given a text prompt y , let the CLIP text encoder output be $\tau_\theta(y) \in \mathbb{R}^{M \times d_\tau}$, M is the number of text tokens, and only the token embedding layer is trainable. Now, for an image x , the VQ-VQE $\varepsilon(\cdot)$ gives a latent representation $z_0 = \varepsilon(x)$. The forward diffusion process gives a noisy latent z_t , where t is uniformly sampled from $\{1, 2, \dots, T\}$. Let $\varphi_i(z_t) \in \mathbb{R}^{N^i \times d_\epsilon^i}$ be the intermediate (flattened) visual representation at layer i corresponding to cross-attention blocks in the denoiser UNet $\epsilon_\theta(\cdot)$, where N^i is the number of visual tokens. The intermediate cross-attention block of UNet maps the text representation onto the image representation for feature generation through the operation

$$\text{Attention}(Q^{(i)}, K^{(i)}, V^{(i)}) = \text{softmax} \left(\frac{Q^{(i)}K^{(i)T}}{\sqrt{d}} \right) V^{(i)}, \quad (2)$$

where $Q^{(i)} = W_Q^{(i)} \cdot \varphi_i(z_t)$, $K^{(i)} = W_K^{(i)} \cdot \tau_\theta(y)$, $V^{(i)} = W_V^{(i)} \cdot \tau_\theta(y)$ are the query, key and value matrices with $W_K^{(i)} \in \mathbb{R}^{d \times d_\tau}$, $W_V^{(i)} \in \mathbb{R}^{d \times d_\tau}$ and $W_Q^{(i)} \in \mathbb{R}^{d \times d_\epsilon^i}$ being the respective projection matrices. Note that, the dot operation shown above in the expansion for Q, K, V is a linear operation and can be expanded as $Q = W_Q \cdot \varphi(z_t) = \varphi(z_t)W_Q^T$.

3.2. Latent Diffusion Models for IQA

Overview: Our work exploits the generalization capabilities of the Stable Diffusion model [29] for IQA by learning cross-attention maps between image and text features in the reverse diffusion process in conjunction with quality-aware prompts to match the visual concepts. In particular, we tap into the reverse diffusion process, where the UNet [30] denoises noisy features. We train the cross-attention modules in the denoising UNet of SDM to maximize the shared information between the visual embeddings captured by the UNet and quality-aware learnable text embeddings generated by the CLIP [27] text encoder. While the cross-attention modules are typically used in SDMs to generate image features consistent with the text input, we utilize such information to measure the alignment between the image features and the text input for IQA. Finally, the

overall quality is a processed output of the cross-attention map computed using the learned text context and the latent image representation.

Learning Quality using Cross-Attention: Our Genz-IQA model involves a joint training of cross-attention key and value weights along with input text embeddings such that the cross-attention map corresponds to the quality estimate. In particular, we adapt the cross-attention module to capture quality-aware representations. We design an IQA model by leveraging this cross-attention mechanism by utilizing the attention map, which projects the text representations onto the images. In particular, we compute the **attention map** at every cross-attention block as

$$A^{(i)} = \text{softmax} \left(\frac{Q^{(i)}K^{(i)T}}{\sqrt{d}} \right), \quad (3)$$

to measure the similarity between the visual query and text key representation. Note that $A^{(i)}$ is used in Eq. 2 to compute the attention output for further processing. In our framework, we learn $W_K^{(i)}$ and $W_V^{(i)}$ since the input text prompts are also learned. We keep $W_Q^{(i)}$ frozen during training as we wish to retain the robust visual information captured by the pretrained model. Note that $A^{(i)}$ is an $N^i \times M$ attention map.

We now perform log-sum-exp (LSE) pooling [2] of the attention map $A^{(i)}$ at every block. As noted in DSD [8], LSE pooling has multi-fold advantages over general average or max pooling, such as robustness to outliers in attention maps and higher stability during training. The predicted quality $g(A)$ using multi-layer attention maps at a particular timestep t for text prompt y is given as,

$$g(A) = \frac{1}{S} \sum_{i=1}^S \frac{1}{M} \sum_{m=1}^M \frac{1}{\lambda} \log \left(\sum_{n=1}^N \exp(\lambda A_{n,m}^{(i)}) \right), \quad (4)$$

where S is the number of cross-attention blocks and $A_{n,m}^{(i)}$ represents the entry at (n, m) in the attention map. λ is a hyperparameter that determines how much to amplify the importance of the most relevant pairs of image and text features. Given the mean opinion score of the image x as MOS, the cost function is

$$\mathcal{L} = \mathbb{E}_{z_t} [(g(A) - \text{MOS})^2], \quad (5)$$

where both the key and value projection matrices of ϵ_θ and the prompt embedding layer of τ_θ are jointly optimized.

We implement LoRA [10] to facilitate finetuning of the cross-attention projection matrices W_K and W_V . Mathematically, for any $W_K \in \mathbb{R}^{d \times d_\tau}$ or $W_V \in \mathbb{R}^{d \times d_\tau}$, the weight update is represented by decomposing them as a product of two low-rank matrices as $W' = W_0 + \Delta W = W_0 + BA$, where $B \in \mathbb{R}^{d \times r}$ and $A \in \mathbb{R}^{r \times d_\tau}$ and rank

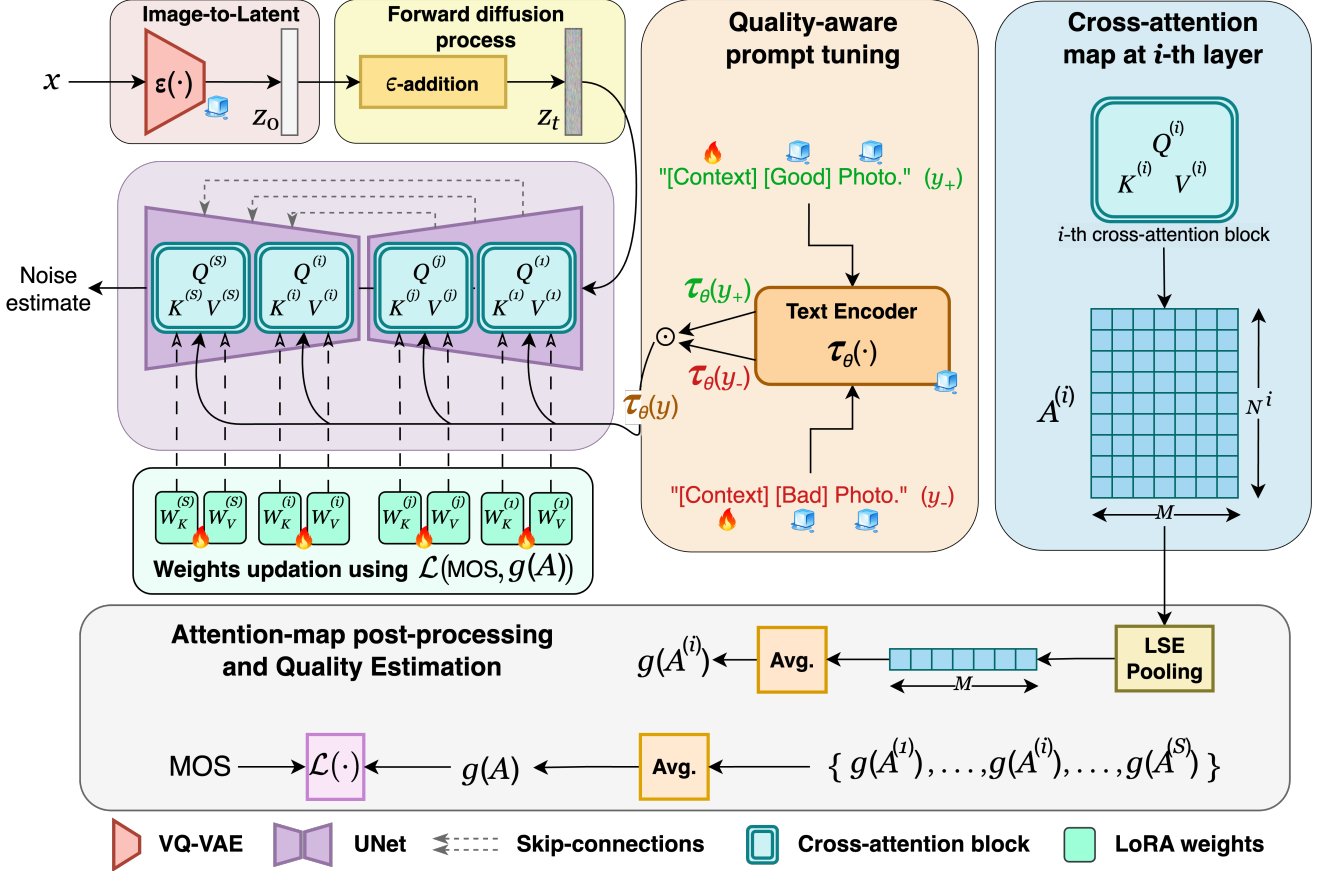


Figure 1: **Overview of GenzIQA framework.** Given an input image x , VQ-VAE processes it to the image latent z_0 . The noisy latent output z_t of the forward diffusion is fed to the denoising UNet [30] $\epsilon_\theta(\cdot)$. At every cross-attention block in $\epsilon_\theta(\cdot)$, the intermediate visual representation is aligned with learnable antonym text representations $\{\tau_\theta(y_+), \tau_\theta(y_-)\}$. After that, the attention maps pooled across cross-attention blocks are used as the predicted quality $g(A)$. Key and Value weight matrices of the cross-attention blocks, along with the learnable context are optimized for $\mathcal{L}(\cdot)$ as in Eq. 5.

$r \ll \min(d, d_\tau)$. During training, LoRA freezes W and only updates BA .

Contextual Prompt Tuning: Although the cross-attention mechanism helps extract quality-aware representations, we further enhance their ability to model quality through prompt-tuning. Prompt-tuning not only saves computational resources but also preserves the generalizable capability of the transformer encoder. Similar to CLIP-IQA⁺, we design an antonym prompt context pair with 'Good Photo', 'Bad Photo' as the initial prompt:

$$\begin{aligned} y_+ &= [\text{Context}] + \text{Positive Attribute}, \\ y_- &= [\text{Context}] + \text{Negative Attribute} \end{aligned} \quad (6)$$

where the $[\text{Context}]$ is a sequence of 16 tokens learned using CoOp [55] while Positive/Negative Attribute here corresponds to the pair 'Good/Bad Photo'. Thus the text input y chosen for the IQA task is given by $\{y_+, y_-\}$. There-

fore, the predicted quality corresponding to $\{y_+, y_-\}$ is given as $g(A^+)$ and $g(A^-)$. We take average of the two quality predictions to estimate the final quality of the given image as we view the two quality predictions as estimates from two diverse quality-aware text prompts.

3.3. Role of Noise in SDM for Quality Estimation

The noise added to the latent features z_0 can have a significant impact on the ability of the SDM to predict image quality. Recall that the denoising UNet of SDM estimates the Gaussian noise incorporated in the forward process. We hypothesize that there is a delicate relationship between the denoising ability of the UNet and the amount of additive noise, which could alter the semantic information and image quality information in the latent image representation. We investigate this by gradually distorting the original image latent z_0 for a fixed length Markov chain. In particular, we generate the images using the pretrained Stable Diffu-

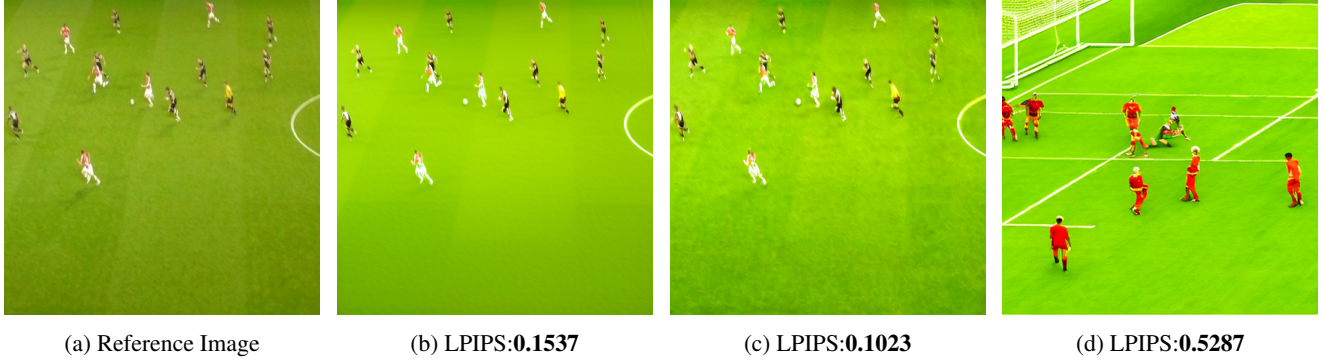


Figure 2: Generated images from zero shot SDM. In Fig. 2b image is generated without noise infused to the image latent, Fig. 2c and Fig. 2d are generated images with noise fed at the timestep $t = 95$ (low noise), and $t = 950$ (high noise) respectively and subsequently denoised. Lower LPIPS scores correspond to better perceptual quality.

sion [29] model with various noise steps in forward diffusion process.

In Fig. 2, we generate images from clean, low noise ($t \in [0 - 100]$) and high noise ($t \in [900 - 1000]$) versions of the original image features. The generated image from the clean latent z_0 in Fig. 2b, is blurry as can be seen from the textureless outfield. This effect maybe attributed to the fact that denoising UNet removes bandpass texture information.

In Fig. 2d, we see that the addition of high Gaussian noise distorts the semantic information in the latent space and thus the UNet generates a content different from the original image. Finally, in Fig. 2c, the image generated preserves both the semantic and texture information as evident visually and from the respective LPIPS scores. In our study, addition of the correct range of noise is extremely important as we wish to capture the perceptual and semantic information at all intermediate stages of the UNet. While the results above indicate a qualitative understanding of the impact of noise on the latent features, we conduct detailed experiments in Sec. 4.6 on the role of noise while using SDM for IQA.

4. Experiments

4.1. Datasets

We perform various experiments on a diverse set of publicly available IQA datasets. **FLIVE** [46] is the largest user-generated content (UGC) dataset comprising diverse crowd-sourced images containing an official train set of 30,253 training and 1.8K test images. We consider two popular in-the-wild image datasets viz. **KonIQ-10K** [9], and **CLIVE** [3] which contain 10,073 and 1,162 samples respectively. **PIPAL** [6] contains around 23,200 restored images produced by 19 different GAN-based algorithms. **NNID** [11] is a nighttime camera-captured database with 1,340 images containing low-light distortions. For various synthetic distortions such as compression, blur, and noise corrupted im-

ages, we choose **LIVE-IQA** [35] and **CSIQ** [17] containing 779 and 866 images respectively. In following sections, we denote KonIQ-10K as **KonIQ**. In our subsequent experiments, we have also used the official test splits of KonIQ and FLIVE, denoted as **KonIQ_{test}** and **FLIVE_{test}** respectively.

4.2. Implementation Details

We choose Stable Diffusion v2 [29] pretrained on LAION-5B [34] dataset with 1.45 billion parameters as our default latent/Stable diffusion model. We choose the model where the VQ-VAE [28] takes in 512×512 image resolution since, in most of the IQA datasets, images are mainly in the range of 360p to 720p. Thus, we resize the images to 512×512 and process the images through the SDM. We freeze all but the key and value weight matrices of the cross-attention blocks in SDM as our goal is to adapt the cross-attention for the quality assessment task. We finetune GenzIQA for 15 epochs with a batch size of 16 and Adam [16] optimizer in different train settings, which are explained in the following sections. We choose the timestep t in the range $(0 - 100]$, and $\lambda = 0.14$ as default based on 7K images of the official validation set of FLIVE. Note that we refer to the noise variance in Eq. 1 through timestep t , implicitly referring to β_t . Also, during training, we choose a single timestep value in the aforementioned range for quality estimation while during testing, the quality is measured as an average over 8 timesteps sampled from the range $(0 - 100]$. We evaluate the GenzIQA model using the Spearman’s Rank Order Correlation Co-efficient (SRCC) and the Pearson’s Linear Correlation Co-efficient (PLCC) between the predicted quality and ground truth human opinion scores.

All experiments were conducted on a 24 GB NVIDIA RTX 3090 GPU with Pytorch 1.13. We accumulate parameter gradients over a batch and thereafter update the model.

Table 1: Performance analysis of GenzIQA with other NR-IQA methods in **cross-database** setting. All the methods are trained on **official FLIVE train** set and tested across various IQA databases.

Methods	Test Database											
	KonIQ		CLIVE		PIPAL		NNID		CSIQ		LIVE-IQA	
	SRCC	PLCC	SRCC	PLCC	SRCC	PLCC	SRCC	PLCC	SRCC	PLCC	SRCC	PLCC
TReS [4]	0.669	0.710	0.729	0.714	0.362	0.359	0.805	0.794	0.587	0.517	0.543	0.445
HyperIQA [38]	0.589	0.635	0.636	0.660	0.304	0.327	0.658	0.651	0.497	0.428	0.514	0.438
MetaIQA [56]	0.578	0.489	0.448	0.410	0.340	0.312	0.452	0.429	0.562	0.536	0.732	0.673
MUSIQ [14]	0.648	0.692	0.662	0.687	0.341	0.331	0.776	0.778	0.484	0.583	0.259	0.335
CLIP-IQA ⁺ [40]	0.724	0.756	0.657	0.673	0.271	0.293	0.694	0.702	0.591	0.617	0.611	0.617
Re-IQA [33]	0.764	0.787	0.699	0.711	0.245	0.266	0.838	0.828	0.324	0.381	0.304	0.338
GRepQ [37]	0.781	0.786	0.736	0.753	0.303	0.318	0.843	0.832	0.579	0.587	0.666	0.568
GenzIQA	0.779	0.823	0.799	0.829	0.473	0.496	0.897	0.878	0.636	0.677	0.789	0.712

4.3. Cross Database Generalization

To study the generalizability of our model, we train GenzIQA with the largest UGC dataset, specifically the official FLIVE train database comprising of 30,253 images.

We evaluate our model on various categories of test datasets such as in-the-wild (KonIQ-10K, CLIVE), GAN-restored images (PIPAL), night-time images (NNID), and synthetically distorted images (CSIQ and LIVE-IQA). We compare with popular state-of-the-art NR-IQA methods in literature such as TReS [4], HyperIQA [38], MetaIQA [56], MUSIQ [14], CLIP-IQA⁺ [40], GRepQ [37], and Re-IQA [33]. We note that all these methods are also trained on the official FLIVE train set for a fair comparison. CLIP-IQA⁺ is an interesting comparison to GenzIQA as it is a vision-language model where learnable prompts are used to estimate quality from the visual and text features. Since LIQE [52] requires detailed annotations of image-text context, we are not able to benchmark LIQE due to the absence of such annotations on the FLIVE [46] dataset. In Tab. 1, we observe that GenzIQA consistently outperforms other benchmarking methods across various cross-database settings. Further, the performance on most databases is acceptable for IQA.

4.4. Analyzing Cross-Attention Map Representation

In this section, we visualize the cross-attention representation of GenzIQA trained on FLIVE to understand why it leads to superior generalization. For this, we subsample good and bad quality images from three different test datasets with MOS less than 30 and greater than 70, respectively. In Fig. 3, we show the 2D tSNE [39] visualization of the cross-attention map in Eq. 3 averaged across all blocks, timestep samples and the number of image tokens. In particular, we chose a perplexity of 40 and iterated the optimization over 1000 steps while generating the tSNE plot. We conclude that the learned attention representation clearly separates high and low-quality images as

evident from Fig. 3. Under similar settings, we also visualize the representation of CLIP-IQA⁺ visual encoder conditioned on the same antonym prompt pair attributes. In particular, the visual feature similarity with antonym text representation gives a 2-dimensional representation for each image. We see that the CLIP-IQA⁺ model’s separability is somewhat inferior to what we see with the cross-attention features of GenzIQA.

4.5. Ablation Study

We evaluate the impact of major components of GenzIQA, particularly the need of cross-attention finetuning, prompt learning, and log-sum exponential (LSE) pooling. In Tab. 2, we report the results of this ablation by training on CLIVE and testing on KonIQ_{test}, FLIVE_{test}, NNID, and LIVE-IQA. The zero-shot performance reported in the first row indicates that all components of GenzIQA are necessary to adapt stable diffusion for IQA.

W/O Cross-Attention. We note from the second row in Tab. 2 that freezing the cross-attention weights severely impact on the overall performance across all databases. This implies that cross-attention text representations (key and value) need to be adapted to capture quality information from the visual query.

W/O Prompt Tuning. As argued in previous works [40] in prompt tuning for QA, we also find that fixing the prompts leads to a significant drop in performance over learnable prompts due to the ambiguity of the fixed prompts in properly conveying perceptual quality related cues.

W/O LSE Pooling. Prior literature [2, 8] shows that LSE pooling gives better performance by providing stability during training and robustness to outliers. We also see such effectiveness due to the inclusion of LSE pooling over average pooling.

4.6. Impact of Noise Level Variation

As discussed in Sec. 3.3, the level of noise added to the image latent space has a direct impact on the abil-

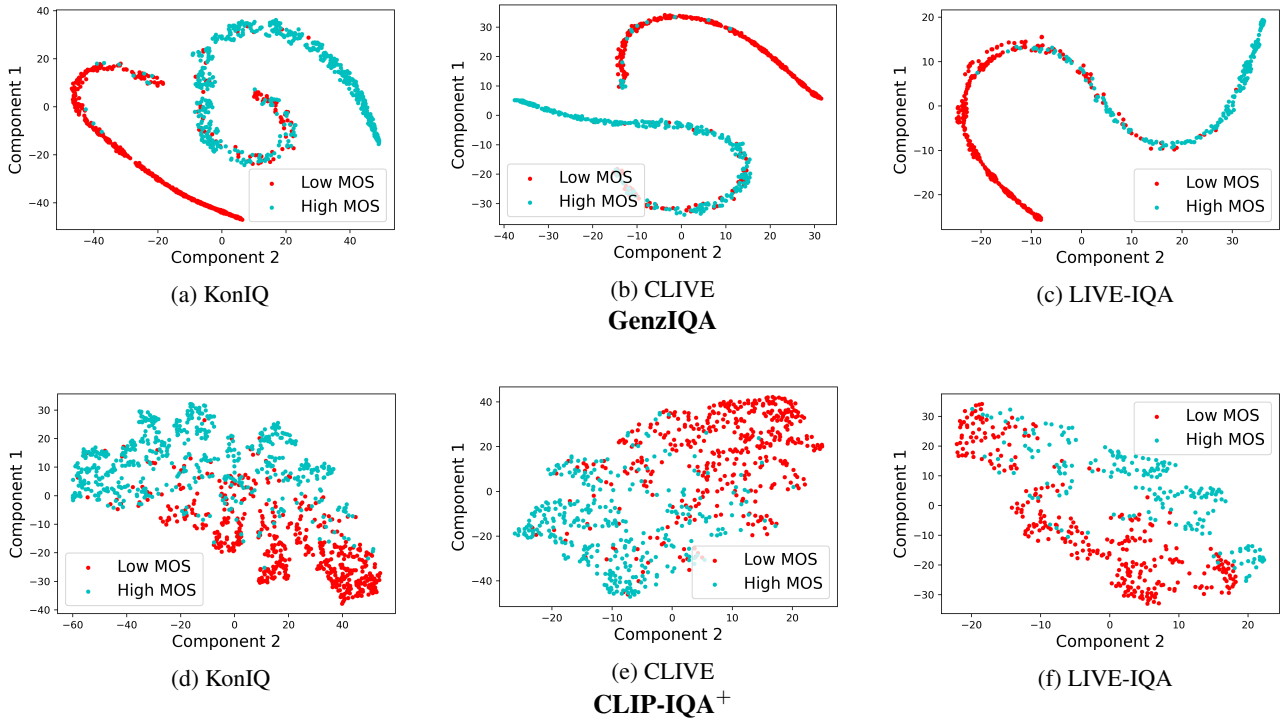


Figure 3: 2D tSNE visualization of cross-attention features of GenzIQA trained on **FLIVE** and tested on images from KonIQ, CLIVE, and LIVE-IQA. CLIP-IQA⁺ similarity features conditioned on antonym prompts are also shown.

Table 2: Ablation study on the impact of various components of GenzIQA trained on **CLIVE** and tested on four datasets. We report the SRCC performance.

Prompt Tuning	Cross Attention	LSE Pooling	KonIQ _{test}	FLIVE _{test}	NNID	LIVE-IQA
×	×	×	0.184	0.010	0.032	0.124
✓	×	✓	0.455	0.284	0.517	0.636
×	✓	✓	0.696	0.331	0.677	0.706
✓	✓	×	0.735	0.438	0.721	0.773
✓	✓	✓	0.750	0.454	0.738	0.782

ity of the denoiser to preserve perceptual information. In this experiment, we train GenzIQA on the CLIVE database with varying levels of noise added to the input. Specifically, we train on CLIVE with timestep in the range $\{0, (0 - 100], [100 - 200], [200 - 300], [400 - 500], [600 - 700], \text{ and } [900 - 1000]\}$. As evident from Fig. 4, the performance across various test datasets is fairly consistent in the range $[0 - 300]$, while it starts to drastically degrade for noisy timesteps beyond 400. This proves our earlier hypothesis that corrupting the image latent with high noise distorts the semantic information, thus hindering the extraction of quality relevant information from the cross-attention map. Further, extremely low noise levels cause blur during de-

noising, leading to poorer quality prediction performance. We see that the $(0, 100]$ range offers a reasonable performance across all datasets.

4.7. Impact of Denoising Steps on Quality Estimation

In Sec. 4.6, we showed that a moderate noise variance is effective while extracting quality features during a single denoising step of reverse diffusion. We now address the complementary question of whether increasing the number of denoising steps and using the latent features from the output after more denoising steps can yield richer features. To understand this, we conduct an experiment where

Table 3: SRCC performance comparison of GenzIQA for different Stable Diffusion variants. Stable Diffusion v2 with two VQ-VAE variants feeding 256×256 and 512×512 sized images are considered.

Resolutions	Train on CLIVE				
	KonIQ _{test}	NNID	CSIQ	LIVE-IQA	FLIVE _{test}
256×256	0.653	0.725	0.567	0.629	0.362
512×512	0.750	0.738	0.664	0.782	0.454
Resolutions	Train on KonIQ				
	CLIVE	NNID	CSIQ	LIVE-IQA	FLIVE _{test}
256×256	0.700	0.776	0.533	0.592	0.445
512×512	0.793	0.782	0.658	0.788	0.489

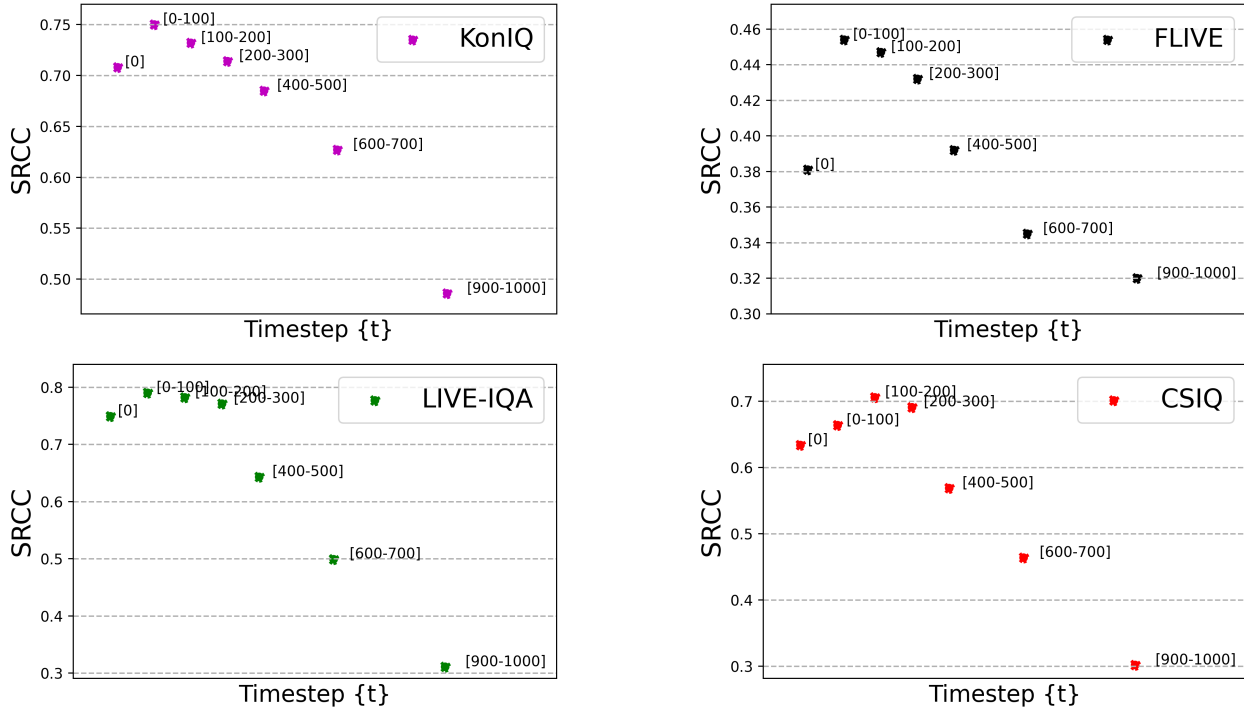


Figure 4: SRCC performance variation of GenzIQA trained on CLIVE and tested across four databases at multiple timesteps.

Table 4: SRCC performance variation of GenzIQA in several steps of a multistep denoising process.

Test database	1st denoising step	3rd denoising step	5th denoising step
KonIQ _{test}	0.747	0.631	0.562
LIVE-IQA	0.782	0.638	0.476
NNID	0.737	0.557	0.417
CSIQ	0.661	0.496	0.415

we let $t \in (0, 100]$ and increase the number of denoising steps from 1 to 5 by reducing t by 20 in each successive step. This reduction of t aligns with how SDM suggests

what noise needs to be added in successive denoising steps. We train the GenzIQA model on the CLIVE dataset and test on multiple datasets for this experiment.

In Tab. 4, we observe that the multi-step denoising performance is always inferior to the single-step denoising performance, and the performance degrades as we tap features from successive denoisers. We believe that since the cross-attention matrices are tuned for quality estimation, this can impact the ability of the denoiser to remove noise for its effective use in successive steps of multi-step denoising. We conclude that it is best to use a single step denoiser to extract quality-aware features from diffusion models.

Table 5: SRCC performance variation of GenzIQA on the choice of prompts being fed as input to the CLIP text encoder. All the variations have been trained on **FLIVE** official train set and cross-tested on these datasets.

Test database	Trainable single prompt	Trainable antonym prompts	Fixed single prompt	Fixed antonym prompts
CLIVE	0.791	0.799	0.784	0.789
NNID	0.880	0.897	0.871	0.874
CSIQ	0.622	0.636	0.568	0.611
LIVE-IQA	0.783	0.789	0.731	0.759

Table 6: Performance comparison of GenzIQA with other NR-IQA methods on Intra-database setting. TReS results from [4] and all other methods except GRepQ from [33].

Methods	FLIVE		KonIQ		CLIVE		LIVE-IQA	
	SRCC	PLCC	SRCC	PLCC	SRCC	PLCC	SRCC	PLCC
TReS [4]	0.554	0.625	0.915	0.928	0.846	0.877	0.969	0.968
HyperIQA [38]	0.535	0.623	0.906	0.917	0.859	0.882	0.962	0.966
DB-CNN [51]	0.554	0.652	0.875	0.884	0.851	0.869	0.968	0.971
CONTRIQUE [22]	0.580	0.651	0.894	0.904	0.845	0.857	0.960	0.961
Re-IQA [33]	0.645	0.733	0.914	0.923	0.840	0.854	0.970	0.971
GRepQ [37]	0.531	0.582	0.908	0.916	0.859	0.867	0.945	0.943
GenzIQA	0.613	0.718	0.916	0.932	0.873	0.897	0.966	0.968

4.8. Different Variants of Stable Diffusion

As argued in the implementation details, we choose the input image resolution to the VQ-VAE as 512×512 since most of the IQA databases have images in the 360p to 720p range. In this section, we analyze the impact of our choice in resolution on quality estimation. In Tab. 3, we study the impact on downscaling by comparing the performance at 512×512 with 256×256 . We train GenzIQA on two different datasets viz. KonIQ and CLIVE and test in a cross-database setting. While training and inference become $4 \times$ faster at 256×256 , the performance drastically deteriorates over all the train-test settings. We conclude that the higher resolution model is a better choice for significant performance gains even though the inference time is slower.

4.9. Study on Learnable Prompt vs Fixed Prompt

GenzIQA by default is trained with learnable antonym prompts using CoOp [55] similar to CLIP-IQA⁺. We study the need for antonym prompts as well as the need for learnable context vectors vs fixed prompts. As argued in [40], antonym prompt pairs are better in estimating quality as we can model the relative difference between the positive and negative quality-aware prompts. In Tab. 5, we choose ['Good Photo.', 'Bad Photo.']. as the initial antonym prompt pair while for the single prompt case, we only choose ['Good Photo.']. We make two observations from this study. Firstly, antonym prompts give a better performance than a single prompt in both the learnable prompt and fixed prompt training across all test

datasets. Secondly, learnable prompts consistently yield superior results with respect to the fixed prompt case. Both these phenomena are expected as multiple studies show the benefit of prompt learning [7, 40, 44], and CLIP-IQA⁺ showed the advantage of antonym prompts in the case of quality.

4.10. Performance on Intra-Database Setting

In this experiment, we validate the performance of our model in intra-database train-test settings. Specifically, we train GenzIQA with either the official train set or the 80% of image samples from various databases and test on the official test set or remaining 20%. In Tab. 6, in case of FLIVE and KonIQ, we train-test on the official split provided, while for CLIVE and LIVE-IQA we randomly split the data 10 times in the ratio 80 : 20 and report the median performance. We infer that our method gives competitive performance with recent state-of-the-art across all databases. We conclude from Tab. 1 and Tab. 6 that GenzIQA not only outperforms recent benchmarks in a practical cross/inter database generalization scenarios but also does remarkably well on intra-database test scenarios.

Run Time: The average test-time required by GenzIQA to estimate quality for a single 512×512 resized image averaged over 8 timesteps on a 24 GB NVIDIA RTX 3090 is **1.4** seconds.

4.11. Limitations

Despite the remarkable ability of SDM to capture visual representations, the pretrained configuration of VQ-VAE re-

Table 7: SRCC performance analysis on the impact of various components of Cross-Attention block in GenzIQA trained on CLIVE and tested on four datasets.

Query Weights	Key Weights	Value Weights	KonIQ _{test}	FLIVE _{test}	NNID	LIVE-IQA
×	×	×	0.455	0.284	0.517	0.636
✓	×	×	0.715	0.410	0.713	0.657
×	✓	✓	0.750	0.454	0.738	0.782
✓	✓	✓	0.750	0.426	0.718	0.752

quires images to be processed at 1 : 1 aspect ratio. Prior work on IQA shows that altering the aspect ratio can have a negative impact on the quality task [47]. Although we achieve the best performance on all the datasets, there is still scope for improvement on PIPAL. We believe that the images in this database are very hard to distinguish in terms of quality and it requires a more fine-grained approach to IQA.

5. Conclusion

In this work, we presented an NR-IQA model by leveraging the benefits of latent diffusion models. Our work is perhaps one of the earliest attempts at understanding whether and how such models can be used for generalized NR-IQA. In this context, it is important to finetune the cross-attention module and learn quality-aware input context vectors to enable the diffusion models be effective for IQA. We believe that GenzIQA will encourage further studies into the use of generative models for superior and practical IQA.

Appendix

A. Impact of Cross-Attention Components

In Sec. 3.2, we kept the weight matrix $W_Q^{(i)}$ of the query for all cross-attention blocks $i \in \{1, 2, \dots, S\}$ frozen as we want to preserve the robust visual information captured by the pre-trained Stable diffusion model. The key and value weights are obtained based on the text prompt, the context of which is also learnt. Thus, we update the key and value weights. In this section, we analyze the impact of freezing query, key and value weights on quality estimation. In Tab. 7, we evaluate GenzIQA trained on CLIVE against four different IQA databases. We infer from the last row that making query weights trainable has an adverse impact on performance. Similarly, freezing the key and value weights also affects the performance.

B. Analysis on Generative Images

In this section, we evaluate the versatility of GenzIQA on various generative image quality databases such as AGIQA-3K [19], AGIQA-1K [53], and AIGCIQA2023 [41]. In par-

Table 8: Performance comparison of GenzIQA with other NR-IQA methods on **generative image databases** in an intra-database setting.

Methods	AGIQA-3K		AGIQA-1K		AIGCIQA	
	SRCC	PLCC	SRCC	PLCC	SRCC	PLCC
CONTRIQUE [22]	0.804	0.868	0.670	0.708	0.809	0.844
Re-IQA [33]	0.785	0.845	0.614	0.670	0.797	0.801
GRepQ [37]	0.808	0.862	0.658	0.708	0.804	0.815
GenzIQA	0.832	0.892	0.840	0.861	0.835	0.859

ticular, we train GenzIQA on 80% samples and test on the remaining 20% over 10 random splits for each of the above databases. We benchmark GenzIQA against other state-of-the-art quality representation learning methods such as CONTRIQUE [22], Re-IQA [33], GRepQ [37] and report the analysis in Tab. 8. We observe that our method performs better than the benchmarks with consistent superior performances across multiple generative IQA databases.

C. Analysis on Choice of Prompts

In our experimental studies, we choose [`'Good Photo.'`, `'Bad Photo.'`] as our initial learnable antonym prompt. As shown in CLIP-IQA+ [40], this prompt pair gives the best estimate of quality. Here, we train GenzIQA with the official FLIVE training set for initial prompts [`'High Quality.'`, `'Low Quality.'`] in Tab. 9, and [`'High Definition.'`, `'Low Definition.'`] in Tab. 10 under different settings. We see that there is minimal variation in performance with respect to the exact choice of these popular quality relevant antonym prompts.

D. Choice of Sampling Timesteps

In Sec. 4, we chose number of sampling timesteps during testing as 8. In Fig. 5, we evaluate GenzIQA trained on the official FLIVE [46] training set on KonIQ [9], CLIVE [3], NNID [11], and LIVE-IQA [35]. We see that number of sampling steps during evaluation marginally increases the performance and saturates at around 8 on all datasets. Thus, we consider the number of sampling steps as 8, although, for faster test-time evaluations, a single sampling timestep

Table 9: SRCC performance variation of GenzIQA trained on FLIVE with **High Quality / Low Quality** as initial prompts.

Test database	Trainable single prompt	Trainable antonym prompts	Fixed single prompt	Fixed antonym prompts
CLIVE	0.776	0.795	0.758	0.761
NNID	0.883	0.889	0.870	0.872
CSIQ	0.616	0.623	0.546	0.576
LIVE-IQA	0.782	0.812	0.734	0.742

Table 10: SRCC performance variation of GenzIQA trained on FLIVE with **High Definition / Low Definition** as initial prompts.

Test database	Trainable single prompt	Trainable antonym prompts	Trainable antonym prompts	Trainable antonym prompts
CLIVE	0.768	0.791	0.752	0.755
NNID	0.880	0.892	0.869	0.871
CSIQ	0.612	0.620	0.548	0.564
LIVE-IQA	0.780	0.800	0.728	0.738

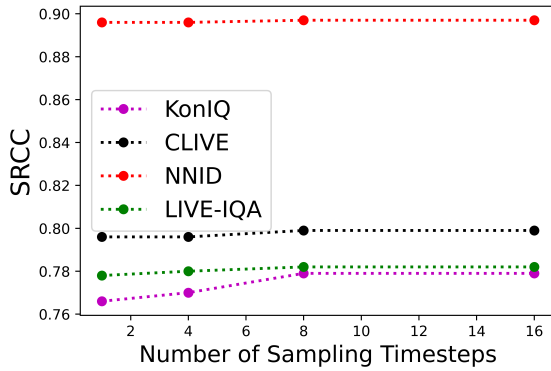


Figure 5: Performance analysis of GenzIQA with varying number of sampling timesteps during evaluation across four test databases.

can also be used.

References

- [1] Žiga Babnik, Peter Peer, and Vitomir Štruc. DifFIQA: Face Image Quality Assessment Using Denoising Diffusion Probabilistic Models. In *Proceedings of the IEEE International Joint Conference on Biometrics (IJCB)*, 2023. 2
- [2] Pierre Blanchard, Desmond J Higham, and Nicholas J Higham. Accurately computing the log-sum-exp and softmax functions. *IMA Journal of Numerical Analysis*, 41(4):2311–2330, 2021. 3, 6
- [3] Deepti Ghadiyaram and Alan C Bovik. Massive online crowdsourced study of subjective and objective picture quality. *IEEE Transactions on Image Processing*, 25(1):372–387, 2015. 5, 10
- [4] S Alireza Golestaneh, Saba Dadsetan, and Kris M Kitani. No-reference image quality assessment via transformers, relative ranking, and self-consistency. In *Proceedings of the IEEE/CVF Winter Conference on Applications of Computer Vision*, pages 1220–1230, 2022. 1, 2, 6, 9
- [5] Ian Goodfellow, Jean Pouget-Abadie, Mehdi Mirza, Bing Xu, David Warde-Farley, Sherjil Ozair, Aaron Courville, and Yoshua Bengio. Generative adversarial networks. *Commun. ACM*, 63(11):139–144, oct 2020. 2
- [6] Jinjin Gu, Haoming Cai, Haoyu Chen, Xiaoxing Ye, Jimmy Ren, and Chao Dong. Pipal: a large-scale image quality assessment dataset for perceptual image restoration. In *European Conference on Computer Vision (ECCV) 2020*, pages 633–651. Springer International Publishing, 2020. 5
- [7] Jiayi Guo, Chaofei Wang, You Wu, Eric Zhang, Kai Wang, Xingqian Xu, Shiji Song, Humphrey Shi, and Gao Huang. Zero-shot generative model adaptation via image-specific prompt learning. In *Proceedings of the IEEE/CVF Conference on Computer Vision and Pattern Recognition (CVPR)*, pages 11494–11503, June 2023. 9
- [8] Xuehai He, Weixi Feng, Tsu-Jui Fu, Varun Jampani, Arjun Akula, Pradyumna Narayana, Sugato Basu, William Yang Wang, and Xin Eric Wang. Discriminative diffusion models as few-shot vision and language learners. *arXiv preprint arXiv:2305.10722*, 2023. 1, 2, 3, 6
- [9] Vlad Hosu, Hanhe Lin, Tamas Sziranyi, and Dietmar Saupe. KonIQ-10k: An ecologically valid database for deep learning of blind image quality assessment. *IEEE Transactions on Image Processing*, 29:4041–4056, 2020. 5, 10
- [10] Edward J Hu, Yelong Shen, Phillip Wallis, Zeyuan Allen-Zhu, Yuanzhi Li, Shean Wang, Lu Wang, and Weizhu Chen. Lora: Low-rank adaptation of large language models. *arXiv preprint arXiv:2106.09685*, 2021. 3
- [11] Runze Hu, Yutao Liu, Zhanyu Wang, and Xiu Li. Blind quality assessment of night-time image. *Displays*, 69:102045, 2021. 5, 10
- [12] Laurynas Karazija, Iro Laina, Andrea Vedaldi, and Christian Rupprecht. Diffusion models for zero-shot open-vocabulary segmentation. *arXiv preprint arXiv:2306.09316*, 2023. 2
- [13] Bahjat Kawar, Shiran Zada, Oran Lang, Omer Tov, Huiwen Chang, Tali Dekel, Inbar Mosseri, and Michal Irani. Imagic: Text-based real image editing with diffusion models. In *Proceedings of the IEEE/CVF Conference on Computer Vision and Pattern Recognition*, pages 6007–6017, 2023. 1
- [14] Junjie Ke, Qifei Wang, Yilin Wang, Peyman Milanfar, and Feng Yang. Musiq: Multi-scale image quality transformer. In *Proceedings of the IEEE/CVF International Conference on Computer Vision*, pages 5148–5157, 2021. 2, 6
- [15] Jongyoo Kim and Sanghoon Lee. Fully deep blind image quality predictor. *IEEE Journal of selected topics in signal processing*, 11(1):206–220, 2016. 2
- [16] Diederik P Kingma and Jimmy Ba. Adam: A method for stochastic optimization. *arXiv preprint arXiv:1412.6980*, 2014. 5
- [17] Eric C Larson and Damon M Chandler. Most apparent distortion: full-reference image quality assessment and the role

- of strategy. *Journal of Electronic Imaging*, 19(1):011006–011006, 2010. 5
- [18] Alexander C Li, Mihir Prabhudesai, Shivam Duggal, Ellis Brown, and Deepak Pathak. Your diffusion model is secretly a zero-shot classifier. *arXiv preprint arXiv:2303.16203*, 2023. 1, 2
- [19] Chunyi Li, Zicheng Zhang, Haoning Wu, Wei Sun, Xiongkuo Min, Xiaohong Liu, Guangtao Zhai, and Weisi Lin. Agiqa-3k: An open database for ai-generated image quality assessment. *arXiv preprint arXiv:2306.04717*, 2023. 10
- [20] Wen Lu, Kai Zeng, Dacheng Tao, Yuan Yuan, and Xinbo Gao. No-reference image quality assessment in contourlet domain. *Neurocomputing*, 73(4-6):784–794, 2010. 1
- [21] Chaofan Ma, Yuhuan Yang, Chen Ju, Fei Zhang, Jinxiang Liu, Yu Wang, Ya Zhang, and Yanfeng Wang. Diffusionseg: Adapting diffusion towards unsupervised object discovery. *arXiv preprint arXiv:2303.09813*, 2023. 1, 2
- [22] Pavan C Madhusudana, Neil Birkbeck, Yilin Wang, Balu Adsumilli, and Alan C Bovik. Image quality assessment using contrastive learning. *IEEE Transactions on Image Processing*, 31:4149–4161, 2022. 1, 2, 9, 10
- [23] Anish Mittal, Anush Krishna Moorthy, and Alan Conrad Bovik. No-reference image quality assessment in the spatial domain. *IEEE Transactions on Image Processing*, 21(12):4695–4708, 2012. 1, 2
- [24] Anish Mittal, Rajiv Soundararajan, and Alan C Bovik. Making a “completely blind” image quality analyzer. *IEEE Signal processing letters*, 20(3):209–212, 2012. 1, 2
- [25] Anush Krishna Moorthy and Alan Conrad Bovik. Blind image quality assessment: From natural scene statistics to perceptual quality. *IEEE Transactions on Image Processing*, 20(12):3350–3364, 2011. 1, 2
- [26] Guanyi Qin, Runze Hu, Yutao Liu, Xiawu Zheng, Haotian Liu, Xiu Li, and Yan Zhang. Data-efficient image quality assessment with attention-panel decoder. In *Proceedings of the AAAI Conference on Artificial Intelligence (AAAI)*, 2023. 1, 2
- [27] Alec Radford, Jong Wook Kim, Chris Hallacy, Aditya Ramesh, Gabriel Goh, Sandhini Agarwal, Girish Sastry, Amanda Askell, Pamela Mishkin, Jack Clark, et al. Learning transferable visual models from natural language supervision. In *International Conference on Machine Learning*, pages 8748–8763. PMLR, 2021. 3
- [28] Ali Razavi, Aaron Van den Oord, and Oriol Vinyals. Generating diverse high-fidelity images with vq-vae-2. *Advances in neural information processing systems*, 32, 2019. 5
- [29] Robin Rombach, Andreas Blattmann, Dominik Lorenz, Patrick Esser, and Björn Ommer. High-resolution image synthesis with latent diffusion models. In *Proceedings of the IEEE/CVF conference on computer vision and pattern recognition*, pages 10684–10695, 2022. 2, 3, 5
- [30] Olaf Ronneberger, Philipp Fischer, and Thomas Brox. U-net: Convolutional networks for biomedical image segmentation. In *Medical Image Computing and Computer-Assisted Intervention–MICCAI 2015: 18th International Conference, Munich, Germany, October 5-9, 2015, Proceedings, Part III 18*, pages 234–241. Springer, 2015. 3, 4
- [31] Subhadeep Roy, Shankhanil Mitra, Soma Biswas, and Rajiv Soundararajan. Test time adaptation for blind image quality assessment. In *Proceedings of the IEEE/CVF International Conference on Computer Vision*, pages 16742–16751, 2023. 2
- [32] Michele A Saad, Alan C Bovik, and Christophe Charrier. Blind image quality assessment: A natural scene statistics approach in the dct domain. *IEEE Transactions on Image Processing*, 21(8):3339–3352, 2012. 2
- [33] Avinab Saha, Sandeep Mishra, and Alan C. Bovik. Re-iqa: Unsupervised learning for image quality assessment in the wild. In *Proceedings of the IEEE/CVF Conference on Computer Vision and Pattern Recognition (CVPR)*, pages 5846–5855, June 2023. 2, 6, 9, 10
- [34] Christoph Schuhmann, Romain Beaumont, Richard Vencu, Cade Gordon, Ross Wightman, Mehdi Cherti, Theo Coombes, Aarush Katta, Clayton Mullis, Mitchell Wortsman, et al. Laion-5b: An open large-scale dataset for training next generation image-text models. *Advances in Neural Information Processing Systems*, 35:25278–25294, 2022. 5
- [35] H.R. Sheikh, M.F. Sabir, and A.C. Bovik. A statistical evaluation of recent full reference image quality assessment algorithms. *IEEE Transactions on Image Processing*, 15(11):3440–3451, 2006. 5, 10
- [36] Ji Shen, Qin Li, and Gordon Erlebacher. Hybrid no-reference natural image quality assessment of noisy, blurry, jpeg2000, and jpeg images. *IEEE Transactions on Image Processing*, 20(8):2089–2098, 2011. 1
- [37] Suhas Srinath, Shankhanil Mitra, Shika Rao, and Rajiv Soundararajan. Learning generalizable perceptual representations for data-efficient no-reference image quality assessment. In *Proceedings of the IEEE/CVF Winter Conference on Applications of Computer Vision*, pages 22–31, 2024. 2, 6, 9, 10
- [38] Shaolin Su, Qingsen Yan, Yu Zhu, Cheng Zhang, Xin Ge, Jinqiu Sun, and Yanning Zhang. Blindly assess image quality in the wild guided by a self-adaptive hyper network. In *Proceedings of the IEEE/CVF Conference on Computer Vision and Pattern Recognition*, pages 3667–3676, 2020. 1, 2, 6, 9
- [39] Zhengzhong Tu, Xiangxu Yu, Yilin Wang, Neil Birkbeck, Balu Adsumilli, and Alan C Bovik. Rapique: Rapid and accurate video quality prediction of user generated content. *IEEE Open Journal of Signal Processing*, 2:425–440, 2021. 6
- [40] Jianyi Wang, Kelvin CK Chan, and Chen Change Loy. Exploring clip for assessing the look and feel of images. In *AAAI*, 2023. 1, 2, 6, 9, 10
- [41] Jiarui Wang, Huiyu Duan, Jing Liu, Shi Chen, Xiongkuo Min, and Guangtao Zhai. Aigcqa2023: A large-scale image quality assessment database for ai generated images: from the perspectives of quality, authenticity and correspondence. In *CAAI International Conference on Artificial Intelligence*, pages 46–57. Springer, 2023. 10
- [42] Weijia Wu, Yuzhong Zhao, Mike Zheng Shou, Hong Zhou, and Chunhua Shen. Diffumask: Synthesizing images with pixel-level annotations for semantic segmentation using diffusion models. *arXiv preprint arXiv:2303.11681*, 2023. 2

- [43] Jingtao Xu, Peng Ye, Qiaohong Li, Haiqing Du, Yong Liu, and David Doermann. Blind image quality assessment based on high order statistics aggregation. *IEEE Transactions on Image Processing*, 25(9):4444–4457, 2016. [2](#)
- [44] Hantao Yao, Rui Zhang, and Changsheng Xu. Visual-language prompt tuning with knowledge-guided context optimization. In *Proceedings of the IEEE/CVF Conference on Computer Vision and Pattern Recognition (CVPR)*, pages 6757–6767, June 2023. [9](#)
- [45] Peng Ye, Jayant Kumar, Le Kang, and David Doermann. Un-supervised feature learning framework for no-reference image quality assessment. In *2012 IEEE conference on Computer Vision and Pattern Recognition*, pages 1098–1105. IEEE, 2012. [1](#), [2](#)
- [46] Zhenqiang Ying, Haoran Niu, Praful Gupta, Dhruv Mahajan, Deepti Ghadiyaram, and Alan Bovik. From patches to pictures (paq-2-piq): Mapping the perceptual space of picture quality. In *Proceedings of the IEEE/CVF Conference on Computer Vision and Pattern Recognition*, pages 3575–3585, 2020. [5](#), [6](#), [10](#)
- [47] Junyong You and Jari Korhonen. Transformer for image quality assessment. In *2021 IEEE International Conference on Image Processing (ICIP)*, pages 1389–1393. IEEE, 2021. [1](#), [2](#), [10](#)
- [48] Hui Zeng, Lei Zhang, and Alan C. Bovik. A probabilistic quality representation approach to deep blind image quality prediction. *CoRR*, abs/1708.08190, 2017. [2](#)
- [49] Lin Zhang, Lei Zhang, and Alan C Bovik. A feature-enriched completely blind image quality evaluator. *IEEE Transactions on Image Processing*, 24(8):2579–2591, 2015. [2](#)
- [50] Richard Zhang, Phillip Isola, Alexei A Efros, Eli Shechtman, and Oliver Wang. The unreasonable effectiveness of deep features as a perceptual metric. In *Proceedings of the IEEE conference on computer vision and pattern recognition*, pages 586–595, 2018. [2](#)
- [51] Weixia Zhang, Kede Ma, Jia Yan, Dexiang Deng, and Zhou Wang. Blind image quality assessment using a deep bilinear convolutional neural network. *IEEE Transactions on Circuits and Systems for Video Technology*, 30(1):36–47, 2018. [1](#), [2](#), [9](#)
- [52] Weixia Zhang, Guangtao Zhai, Ying Wei, Xiaokang Yang, and Kede Ma. Blind image quality assessment via vision-language correspondence: A multitask learning perspective. In *Proceedings of the IEEE/CVF Conference on Computer Vision and Pattern Recognition*, pages 14071–14081, 2023. [2](#), [6](#)
- [53] Zicheng Zhang, Chunyi Li, Wei Sun, Xiaohong Liu, Xionghuo Min, and Guangtao Zhai. A perceptual quality assessment exploration for aigc images. *arXiv e-prints*, pages arXiv–2303, 2023. [10](#)
- [54] Kai Zhao, Kun Yuan, Ming Sun, Mading Li, and Xing Wen. Quality-aware pre-trained models for blind image quality assessment. In *Proceedings of the IEEE/CVF Conference on Computer Vision and Pattern Recognition*, pages 22302–22313, 2023. [2](#)
- [55] Kaiyang Zhou, Jingkang Yang, Chen Change Loy, and Ziwei Liu. Learning to prompt for vision-language models. *International Journal of Computer Vision*, 130(9):2337–2348, 2022. [4](#), [9](#)
- [56] Hancheng Zhu, Leida Li, Jinjian Wu, Weisheng Dong, and Guangming Shi. MetaIqa: Deep meta-learning for no-reference image quality assessment. In *Proceedings of the IEEE/CVF Conference on Computer Vision and Pattern Recognition*, pages 14143–14152, 2020. [1](#), [2](#), [6](#)